

Metastable interwoven mesoporous metal-organic frameworks

Yabing He,^{†‡} Zhiyong Guo,[‡] Shengchang Xiang,[§] Zhangjing Zhang,[§] Wei Zhou,[≠] Frank R. Fronczek,¹ Sean Parkin,[‡] Stephen T. Hyde,[◇] Michael O’Keeffe,[△] and Banglin Chen^{*‡}.

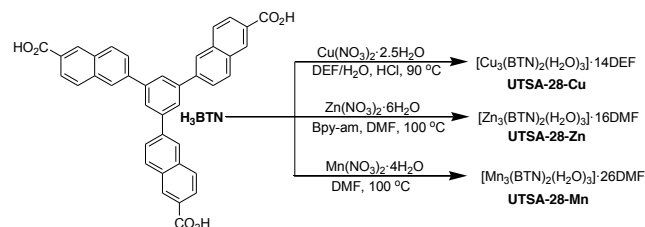
[†]College of Chemistry and Life Sciences, Zhejiang Normal University, Jinhua 321004, China; [‡]Department of Chemistry, University of Texas at San Antonio, One UTSA Circle, San Antonio, Texas 78249-0698, United States; [§]College of Chemistry and Material, Fujian Normal University, 3 Shangsang Road, Cangshang Region, Fuzhou 350007, China; [≠]NIST Center for Neutron Research, Gaithersburg, Maryland 20899-6102, United States; [‡]Department of Materials Science and Engineering, University of Maryland, College Park, Maryland 20742, United States; ¹Department of Chemistry, Louisiana State University, Baton Rouge, LA 70803-1804, United States; [†]Department of Chemistry, University of Kentucky, Lexington, KY, 40506-0055, United States; [◇]Department of Applied Mathematics, Australian National University, Canberra, Australia; [△]Department of Chemistry and Biochemistry, Arizona State University Tempe, Arizona 85287-1604, United States.

Supporting Information Placeholder

ABSTRACT: Three isostructural interwoven (3,4)-connected mesoporous metal-organic frameworks of **pto-a** topology (UTSA-28-Cu, UTSA-28-Zn, and UTSA-28-Mn) were synthesized and structurally characterized. Because of their metastable nature, their gas sorption properties are highly dependent on the metal ions and activation profiles. The most stable UTSA-28a-Cu exhibits high gas storage capacities.

Metal-organic frameworks (MOFs) and/or porous coordination polymers (PCPs) are a new class of porous materials which have been widely studied not only for their fascinating structures but more importantly for their diverse applications in gas storage and separation, catalysis, sensing and drug delivery.^{1,2} The establishment of their permanent porosities is necessary for us to explore the above mentioned properties, thus extensive research has been pursued to stabilize the frameworks. Unlike the ionic bonds in the sophisticated zeolite porous materials, the coordination bonds to generate the MOFs are much weaker, leading to their unique structure features such as framework flexibility and metastability. Because of these, the establishment of their permanent porosities is not only dependent on their structures, but also dependent on the activation profiles, particularly for those mesoporous MOFs.³ In fact, a few mesoporous MOFs whose gas sorption cannot be established through conventional activation have been confirmed to take up large amount of gas molecules through the activation with supercritical carbon dioxide (SCD).⁴ We report herein three isostructural interwoven mesoporous metal-organic frameworks UTSA-28-Cu, UTSA-28-Zn, and UTSA-28-Mn which are assembled from the new BTN linker ($H_3BTN = 6,6',6''$ -benzene-1,3,5-triyl-2,2',2''-trinaphthoic acid, Scheme 1) and binuclear $M_2(CO_2)_4$ ($M = Cu^{2+}$, Zn^{2+} and Mn^{2+}) paddlewheel secondary building units (SBUs). This new expanded BTB ($H_3BTB = 4,4',4''$ -benzene-1,3,5-triyl-tribenzoic acid) organic

Scheme 1. Synthesis of MOFs.



linker has enlarged the cages of 16.4 Å in MOF-14 ($Cu_3(BTB)_2(H_2O)_3$)⁵ into the ones of 25.6 Å in UTSA-28. More interestingly, this series of mesoporous MOFs exhibit framework meta-stability attributed to their interwoven structures, so their permanent porosities are not only dependent on the metal ions but also dependent on the activation profiles. The establishment of high porosity (BET = 3179 m²/g) of the UTSA-28a-Cu has enabled it to take a large amount of CH₄ (total of 197.3 cm³ (STP)/g at 300 K and 46 bar) and CO₂ (total of 413 cm³ (STP)/g at 300 K and 28 bar).

The C₃-symmetric organic linker H₃BTN was readily synthesized by Pd-catalyzed Suzuki cross-coupling between 1,3,5-tribromobenzene and methyl 6-(pinacolboronyl)-2-naphthoate followed by hydrolysis and acidification in good yield. Solvothermal reaction between H₃BTN and Cu(NO₃)₂·2.5H₂O in *N,N*-diethylformamide (DEF)/H₂O mixture under acidic conditions at 90 °C for 24 h afforded blue polyhedral-shaped single crystals of UTSA-28-Cu ($[Cu_3(BTN)_2(H_2O)_3]·14DEF$). UTSA-28-Zn ($[Zn_3(BTN)_2(H_2O)_3]·16DMF$) was obtained as colorless block-shaped crystals via a solvothermal reaction between H₃BTN and Zn(NO₃)₂·6H₂O in *N,N*-dimethylformamide (DMF) in the presence of *N*-(pyridin-4-yl)isonicotinamide (Bpy-am); while UTSA-28-Mn ($[Mn_3(BTN)_2(H_2O)_3]·26DMF$) was synthesized by a solvothermal reaction of H₃BTN and Mn(NO₃)₂·4H₂O in DMF for one week. Their structures were determined by single-crystal X-ray diffraction analysis, and

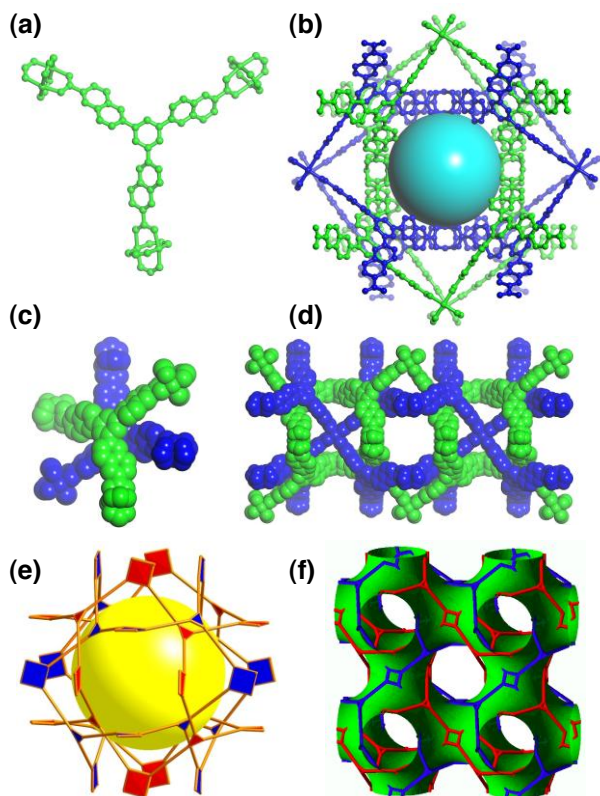


Figure 1. Single-crystal X-ray structure of UTSA-28-Cu indicating that square $\text{Cu}_2(\text{CO}_2)_4$ SBUs were linked by triangular BTN units (a) to form a pair of interwoven frameworks (b) with **pto-a** topology (e) that are held together by numerous π - π and CH - π interactions (c and d) on the P-surface (f).

the phase purity of the bulk materials was confirmed by powder X-ray diffraction (PXRD, Fig. S1-3, ESI). The formulae were established based on single-crystal X-ray diffraction studies, thermogravimetric analysis (TGA, Fig. S4) and microanalysis.

Since the single-crystal X-ray studies and PXRD experiments confirm that they are isostructural, the crystal structure of UTSA-28-Cu was representatively described. UTSA-28-Cu is an interwoven 3D framework that crystallized in a cubic space group $Pn\bar{3}n$. Each framework is composed of *in situ* formed $\text{Cu}_2(\text{CO}_2)_4$ SBUs which are linked by triangular BTN units to form a (3,4)-connected net with the **pto** topology (Fig. 1a-b),⁵ where the BTN units serve as a 3-connected node and the $\text{Cu}_2(\text{CO}_2)_4$ SBUs serve as a planar 4-connected node. The naphthalene ring in the organic linker is twisted from the center benzene ring with a dihedral angle of 36.5° . A pair of frameworks are interwoven each other on the P-surface with the center to center distance of 3.9 \AA between the center benzene ring of BTN (Fig. 1c-f). Because the BTN is larger than BTB, the cages of 25.6 \AA in UTSA-28-Cu are larger than the ones of 16.4 \AA in MOF-14.⁶ Accordingly, UTSA-28-Cu also has larger effective window sizes of about $11.1 \times 11.1 \text{ \AA}^2$. The total accessible volume in UTSA-28-Cu was calculated using PLATON to be 77% after removal of guest solvents and coordinated water molecules.⁷

Different activation methods were used to determine the permanent porosity by nitrogen adsorption at 77 K. The as-synthesized UTSA-28-Cu was guest-exchanged with dry ace-

tone, dichloromethane, and methanol, respectively, and then followed by the activation at room temperature under high vacuum overnight to get the activated UTSA-28a-Cu, UTSA-28b-Cu and UTSA-28c-Cu, respectively. UTSA-28d-Cu was prepared through the freeze drying activation in which the freshly benzene-exchanged UTSA-28-Cu was activated under high vacuum at 0°C overnight followed by at room temperature for 24 hrs.⁸

The N_2 sorption isotherms of all activated samples are shown in Fig. 2a, and the corresponding BET and Langmuir surface areas as well as pore volumes are listed in Table S1. The significantly different N_2 sorption isotherms of these samples are attributed to the metastable nature of UTSA-28-Cu. The most surprising are the facts that UTSA-28c-Cu and UTSA-28d-Cu, generated from the freshly methanol and benzene exchanged samples, respectively, do not take up any N_2 molecules at all. The exact reason is not very clear; we speculate that the strong interactions between the guest methanol molecules with the framework (particularly the terminal water molecules) among the UTSA-28c-Cu, and the strong aromatic π - π interactions between the guest benzene molecules with the BTN organic linkers within the

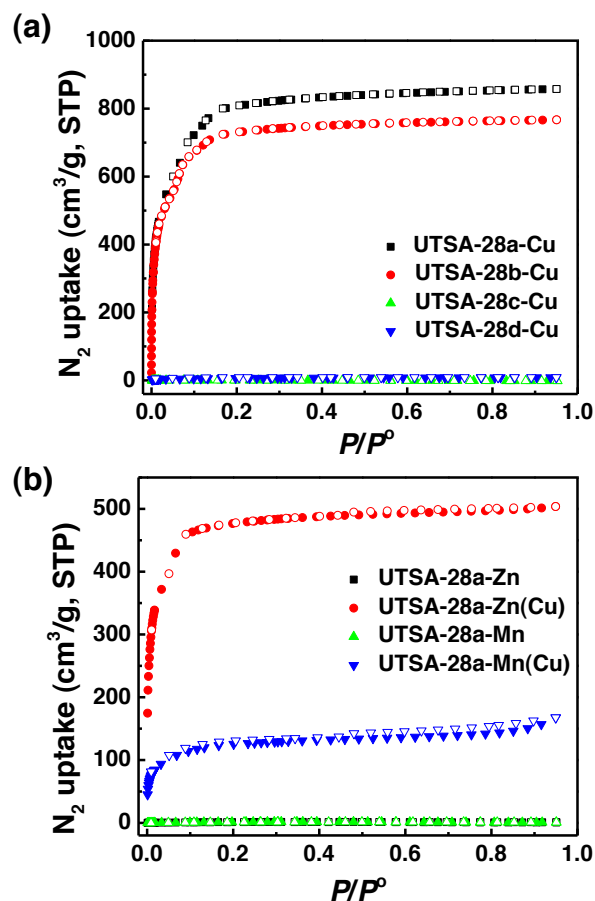


Figure 2. N_2 sorption isotherms at 77 K for (a) the activated UTSA-28a-Cu, UTSA-28b-Cu, UTSA-28c-Cu, and UTSA-28d-Cu, and for (b) the activated UTSA-28a-Zn, UTSA-28a-Mn, UTSA-28a-Zn(Cu) and UTSA-28a-Mn(Cu). The solid and open symbols represent the adsorption and desorption data, respectively.

framework UTSA-28d-Cu play a crucial role. Using acetone as activation solvent produced the most porous framework:

the activated UTSA-28a-Cu exhibits the Brunauer-Emmett-Teller (BET) and Langmuir surface areas of 3179 and 3957 m^2/g , respectively. These values are about twice as the ones in MOF-14.⁶ The pore volume calculated from the maximum amount of N_2 adsorbed is 1.33 cm^3/g .

It is understandable that UTSA-28a-Zn and UTSA-28a-Mn do not take up any N_2 molecules because the $\text{Zn}_2(\text{CO}_2)_4$ and $\text{Mn}_2(\text{CO}_2)_4$ SBUs are not as rigid as the $\text{Cu}_2(\text{CO}_2)_4$ one to stabilize the frameworks. In fact, even the HKUST-1 analogy $\text{Zn}_3(\text{BTC})_2$ is not porous at all.⁹ Inspired by the recent reports that the $\text{Zn}_2(\text{CO}_2)_4$ SBUs in a MOF can be substituted by the $\text{Cu}_2(\text{CO}_2)_4$ ones *via* post-synthetic metal ion exchange,¹⁰ we prepared the Cu(II) substituted UTSA-28-Zn and UTSA-28-Mn, namely UTSA-28-Zn(Cu) and UTSA-28-Mn(Cu), respectively. When the as-synthesized UTSA-28-Zn were immersed in a 0.1 M methanol solution of $\text{Cu}(\text{NO}_3)_2 \cdot 2.5\text{H}_2\text{O}$ at room temperature for one week, the original colorless crystals turned into green blue ones while maintaining their original shapes and sizes (Fig. S6), indicating a clean single-crystal to single-crystal (SCSC) transformation. Inductively coupled plasma (ICP) analysis of the metal ion exchanged sample UTSA-28-Zn(Cu) indicates that up to 80% of Zn ions in the framework were exchanged by Cu ions over one week. The PXRD studies confirmed that the framework was preserved during the metal ion exchange process (Fig. S7). In addition, no stretching band corresponding to nitrate anion was detected in FTIR spectra of UTSA-28-Zn(Cu), demonstrating that there was no Cu(II) ion absorbed in the pore channels (Fig. S8). The acetone exchanged UTSA-28-Zn(Cu) was activated under vacuum at room temperature to investigate its porosity. Remarkably, UTSA-28a-Zn(Cu) shows a significantly improved gas sorption properties compared to the original UTSA-28a-Zn (Fig. 2b, Table S1). N_2 uptake of UTSA-28a-Zn(Cu) reaches 504 cm^3/g at 1 atm at 77 K, corresponding to the BET surface area of 1890 m^2/g . The permanent porosity of the activated UTSA-28a-Mn(Cu) has been also established (Fig. 2b, Table S1).

Establishment of permanent porosity of UTSA-28a-Cu encourages us to explore its gas storage and separation capacities. Because of its high porosities, the high-pressure CO_2 , CH_4 and H_2 adsorptions up to 60 bar were measured at the Center for Neutron Research, National Institute of Standards and Technology (NIST) using a computer-controlled Sieverts apparatus (Fig. 3a). The H_2 adsorption isotherm of UTSA-28a-Cu shows a maximum excess uptake of 3.9 wt% at 33 bar and 77 K (Fig. S9a). By using the N_2 derived pore volume and the bulk phase density of H_2 , the total H_2 uptake at 77 K and 52 bar was calculated to be 5.0 wt% (Fig. S9b), which is moderate compared with the highest capacity MOF materials.⁴ At 35 bar and 300 K, the excess and absolute CH_4 uptakes of UTSA-28a-Cu reach 149.2 and 167.9 cm^3 (STP)/g, respectively. The total methane uptake can increase to 197.3 cm^3 (STP)/g at 300 K and 46 bar (Fig. 3a and Fig. S10). The total CO_2 adsorption capacity is 81.1 wt% (413 cm^3 (STP)/g) at 300 K and 28 bar (Fig. 3a and Fig. S11), which are moderately high.

We have recently paid much attention to porous MOFs for the storage and separation of small hydrocarbons because of their very important industrial applications.¹¹ Accordingly,

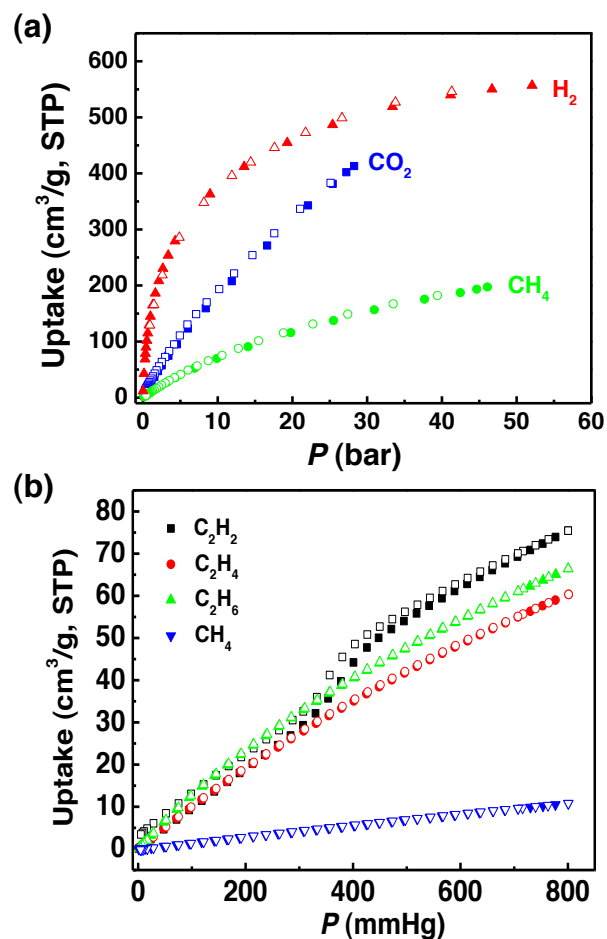


Figure 3. (a) Absolute high-pressure CO_2 (300 K), CH_4 (300 K) and H_2 (77 K) sorption isotherms of UTSA-28a-Cu. (b) C_2H_2 , C_2H_4 , C_2H_6 , and CH_4 sorption isotherms of UTSA-28a-Cu at 296 K. The solid and open symbols represent the adsorption and desorption data, respectively.

the pure-component small hydrocarbon sorption isotherms for UTSA-28a-Cu were measured. As shown in Fig. 3b and Fig. S12, all isotherms show reversible type-I sorption behavior. Remarkably, UTSA-28a-Cu systematically takes up much more C_2 hydrocarbons than C_1 methane. At 296 K, UTSA-28a-Cu take up a moderate amount of C_2H_2 , C_2H_4 , and C_2H_6 , but basically a negligible amount of CH_4 at 1 atm, indicating UTSA-28a-Cu as a promising material for adsorptive separation of C_2 hydrocarbons from methane at room temperature. The Henry's law selectivities for C_2H_2 , C_2H_4 , and C_2H_6 over CH_4 at 296 K are 9.2, 8.6 and 13.2, respectively, which are moderate compared with the best performing materials FeMOF-74, CoMOF-74 and MgMOF-74.^{11a,12} Nevertheless, the low isosteric heat of adsorption at zero coverage (16.9-25.6 kJ mol^{-1} , Table S2), calculated by fitting experimental isotherm data at 273 K and 296 K to the virial equation, indicates the low regeneration cost. The large pore volume of the UTSA-28a-Cu will also secure its large separation capacities for the small hydrocarbons. In practical applications, both separation selectivity and capacity should be balanced to optimize the separation efficiency.

In summary, we synthesized three isostructural interwoven metal-organic frameworks based on a new C_3 -symmetrical aromatic tricarboxylate of the **pto-a** topology.

The large pore space of 25.6 Å in mesoporous regime and weak interactions between the two interwoven frameworks lead to their metastable structure features, so their framework stability and gas sorption properties were heavily dependent on the metal ions and the activation profiles. The most stable UTSA-28a-Cu exhibits the potential for gas storage and separation. Our work thus demonstrates the significance of activation profiles on the controlling the framework stability and porosity.

ASSOCIATED CONTENT

Supporting Information

Experimental details, PXRD patterns, TGA data, FTIR spectra, gas sorption isotherms, and virial analysis. This material is available free of charge via the Internet at <http://pubs.acs.org>.

AUTHOR INFORMATION

Corresponding Author

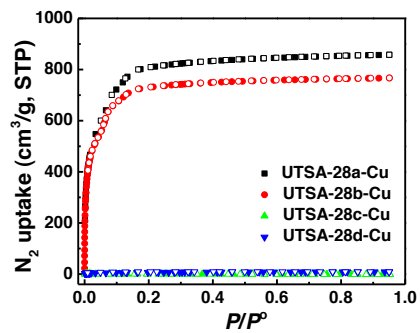
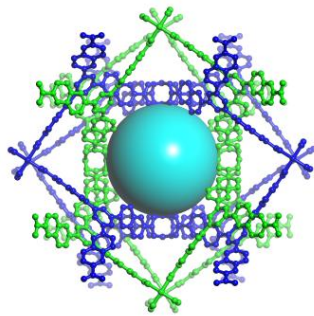
banglin.chen@utsa.edu.

ACKNOWLEDGMENT

This work was supported by Award AX-1730 from the Welch Foundation (B.C.).

REFERENCES

- (1) (a) He, Y.; Zhou, W.; Krishna, R.; Chen, B. *Chem. Commun.* **2012**, 48, 11813. (b) Suh, M. P.; Park, H. J.; Prasad, T. K.; Lim, D.-W. *Chem. Rev.* **2012**, 112, 782. (c) Lin, X.; Champness, N. R.; Schröder, M. *Top. Curr. Chem.* **2010**, 293, 35. (d) Ma, S.; Zhou, H.-C. *Chem. Commun.* **2010**, 46, 44. (e) Makal, T. A.; Li, J.-R.; Lu, W.; Zhou, H.-C. *Chem. Soc. Rev.* **2012**, 41, 7761. (f) Getman, R. B.; Bae, Y.-S.; Wilmer, C. E.; Snurr, R. Q. *Chem. Rev.* **2012**, 112, 703. (g) Li, J.-R.; Sculley, J.; Zhou, H.-C. *Chem. Rev.* **2012**, 112, 869. (h) Sumida, K.; Rogow, D. L.; Mason, J. A.; McDonald, T. M.; Bloch, E. D.; Herm, Z. R.; Bae, T.-H.; Long, J. R. *Chem. Rev.* **2012**, 112, 724. (i) Wu, H.; Gong, Q.; Olson, D. H.; Li, J. *Chem. Rev.* **2012**, 112, 836. (j) Yoon, M.; Srirambalaji, R.; Kim, K. *Chem. Rev.* **2012**, 112, 1196. (k) Chen, B.; Xiang, S.; Qian, G. *Acc. Chem. Res.* **2010**, 43, 1115. (l) Cui, Y.; Yue, Y.; Qian, G.; Chen, B. *Chem. Rev.* **2012**, 112, 1126. (m) Kreno, L. E.; Leong, K.; Farha, O. K.; Allendorf, M.; Dwyne, R. P. V.; Hupp, J. T. *Chem. Rev.* **2012**, 112, 1105. (n) Allendorf, M. D.; Bauer, C. A.; Bhakta, R. K.; Houk, R. J. T. *Chem. Soc. Rev.* **2009**, 38, 1330. (o) Horcajada, P.; Gref, R.; Baati, T.; Allan, P. K.; Maurin, G.; Couvreur, P.; Férey, G.; Morris, R. E.; Serre, C. *Chem. Rev.* **2012**, 112, 1232. (p) Kitagawa, S.; Kitaura, R.; Noro, S.-i. *Angew. Chem. Int. Ed.* **2004**, 43, 2334. (q) Yaghi, O. M.; O'Keeffe, M.; Ockwig, N. W.; Chae, H. K.; Eddaoudi, M.; Kim, J. *Nature* **2003**, 423, 705.
- (2) (a) Nugent, P.; Belmabkhout, Y.; Burd, S. D.; Cairns, A. J.; Luebke, R.; Forrest, K.; Pham, T.; Ma, S.; Space, B.; LukaszWojtas; Eddaoudi, M.; Zaworotko, M. J. *Nature* **2013**, 495, 80. (b) Vaidhyanathan, R.; Iremonger, S. S.; Shimizu, G. K. H.; Boyd, P. G.; Alavi, S.; Woo, T. K. *Science* **2010**, 330, 650. (c) Xue, D.-X.; Cairns, A. J.; Belmabkhout, Y.; Wojtas, L.; Liu, Y.; Alkordi, M. H.; Eddaoudi, M. *J. Am. Chem. Soc.* **2013**, 135, 7660-7667. (d) Caskey, S. R.; Wong-Foy, A. G.; Matzger, A. J. *J. Am. Chem. Soc.* **2008**, 130, 10870. (e) Gedrich, K.; Senkowska, I.; Klein, N.; Stoeck, U.; Henschel, A.; Lohe, M. R.; Baburin, I. A.; Mueller, U.; Kaskel, S. *Angew. Chem. Int. Ed.* **2010**, 49, 8489. (f) Panda, T.; Pachfule, P.; Chen, Y.; Jiang, J.; Banerjee, R. *Chem. Commun.* **2011**, 47, 2011. (g) Lin, Q.; Wu, T.; Zheng, S.-T.; Bu, X.; Feng, P. *J. Am. Chem. Soc.* **2012**, 134, 784. (h) Zhang, J.-P.; Chen, X.-M. *J. Am. Chem. Soc.* **2009**, 131, 5516. (i) Jiang, H.-L.; Xu, Q. *Chem. Commun.* **2011**, 47, 3351. (j) Wu, H.; Zhou, W.; Yildirim, T. *J. Am. Chem. Soc.* **2009**, 131, 4995. (k) He, Y.; Zhou, W.; Yildirim, T.; Chen, B. *Energy Environ. Sci.* **2013**, 6, DOI: 1039/C3EE41166D.
- (3) (a) Fang, Q.-R.; Makal, T. A.; Young, M. D.; Zhou, H.-C. *Comment. Inorg. Chem.* **2010**, 31, 165. (b) Xuan, W.; Zhu, C.; Liu, Y.; Cui, Y. *Chem. Soc. Rev.* **2012**, 41, 1677. (c) Song, L.; Zhang, J.; Sun, L.; Xu, F.; Li, F.; Zhang, H.; Si, X.; Jiao, C.; Li, Z.; Liu, S.; Liu, Y.; Zhou, H.; Sun, D.; Du, Y.; Cao, Z.; Gabelica, Z. *Energy Environ. Sci.* **2012**, 5, 7508.
- (4) (a) Farha, O. K.; Yazaydin, A. Ö.; Eryazici, I.; Malliakas, C. D.; Hauser, B. G.; Kanatzidis, M. G.; Nguyen, S. T.; Snurr, R. Q.; Hupp, J. T. *Nature Chem.* **2010**, 2, 944. (b) Furukawa, H.; Ko, N.; Go, Y. B.; Aratani, N.; Choi, S. B.; Choi, E.; Yazaydin, A. Ö.; Snurr, R. Q.; O'Keeffe, M.; Kim, J.; Yaghi, O. M. *Science* **2010**, 329, 424.
- (5) O'Keeffe, M.; Peskov, M. A.; Ramsden, S. J.; Yaghi, O. M. *Acc. Chem. Res.* **2008**, 41, 1782.
- (6) Chen, B.; Eddaoudi, M.; Hyde, S. T.; O'Keeffe, M.; Yaghi, O. M. *Science* **2001**, 291, 1021.
- (7) Spek, A. L. PLATON, a multipurpose crystallographic tool, Utrecht University, Utrecht, The Netherlands, **2001**.
- (8) (a) Ma, L.; Jin, A.; Xie, Z.; Lin, W. *Angew. Chem. Int. Ed.* **2009**, 48, 9905. (b) He, Y.-P.; Tan, Y.-X.; Zhang, J. *Inorg. Chem.* **2012**, 51, 11232.
- (9) (a) Feldblyum, J. I.; Liu, M.; Gidley, D. W.; Matzger, A. J. *J. Am. Chem. Soc.* **2011**, 133, 18257. (b) Wade, C. R.; Dincă, M. *Dalton Trans.* **2012**, 41, 7931.
- (10) (a) Das, S.; Kim, H.; Kim, K. *J. Am. Chem. Soc.* **2009**, 131, 3814. (b) Prasad, T. K.; Hong, D. H.; Suh, M. P. *Chem. Eur. J.* **2010**, 16, 14043. (c) Wei, Z.; Lu, W.; Jiang, H.-L.; Zhou, H.-C. *Inorg. Chem.* **2013**, 52, 1164-1166. (d) Wang, X.-J.; Li, P.-Z.; Liu, L.; Zhang, Q.; Borah, P.; Wong, J. D.; Chan, X. X.; Rakesh, G.; Li, Y.; Zhao, Y. *Chem. Commun.* **2012**, 48, 10286-10288.
- (11) (a) He, Y.; Krishna, R.; Chen, B. *Energy Environ. Sci.* **2012**, 5, 9107. (b) He, Y.; Zhang, Z.; Xiang, S.; Fronczek, F. R.; Krishna, R.; Chen, B. *Chem. Eur. J.* **2012**, 18, 613. (c) He, Y.; Zhang, Z.; Xiang, S.; Fronczek, F. R.; Krishna, R.; Chen, B. *Chem. Commun.* **2012**, 48, 6493. (d) He, Y.; Xiang, S.; Zhang, Z.; Xiong, S.; Fronczek, F. R.; Krishna, R.; O'Keeffe, M.; Chen, B. *Chem. Commun.* **2012**, 48, 10856. (e) Xiang, S.; Zhang, Z.; Zhao, C.-G.; Hong, K.; Zhao, X.; Ding, D.-L.; Xie, M.-H.; Wu, C.-D.; Gill, R.; Thomas, K. M.; Chen, B. *Nature Commun.* **2012**, 2, 204. (f) Das, M. C.; Guo, Q.; He, Y.; Kim, J.; Zhao, C.-G.; Hong, K.; Xiang, S.; Zhang, Z.; Thomas, K. M.; Krishna, R.; Chen, B. *J. Am. Chem. Soc.* **2012**, 134, 8703. (g) Zhang, Z.; Xiang, S.; Chen, B. *CrystEngComm* **2011**, 13, 5983.
- (12) Bloch, E. D.; Queen, W. L.; Krishna, R.; Zdrozny, J. M.; Brown, C. M.; Long, J. R. *Science* **2012**, 335, 1606.



A series of interwoven mesoporous metal-organic frameworks were structurally characterized and examined for their gas sorption, underlying their metastable structure feature.
